DISTRIBUTION OF VERTICAL LOADS BETWEEN INTERCONNECTED MASONRY WALLS WITH AND WITHOUT A TOP SLAB

V. CAPUZZO NETO [(1)]; M.R.S. CORRÊA[(2)]; M.A. RAMALHO[(3)]

[1] Lecturer – Federal Technical School of Palmas – Tocantins – Brazil – capuzzo@etfto.gov.br
[2] Associate Professor - University of Sao Paulo – Sao Paulo – Brazil – mcorrea@sc.usp.br
[3] Associate Professor - University of Sao Paulo – Sao Paulo – Brazil – ramalho@sc.usp.br

SUMMARY

An experimental study of the structural interaction of running bond interconnected walls subjected to vertical loading is presented, showing the influence of a top slab on the load capacity of H-panels.

INTRODUCTION

In order for the development of a structural design of a building to be successful, it has to provide a good representation of the stress paths throughout the whole structure. However, the distribution of vertical loads between interconnected walls of a masonry building is not yet well understood. A key point is the interaction of interconnected walls. The degree of interaction depends on the geometric properties of the walls, the existence of a top slab and the way the walls are bonded, as well as the occurrence of bond beams. The composite behaviour depends on the capacity of the common interface to transfer the interaction forces.

There are few research projects dealing with experiments to evaluate shear strength at vertical wall interfaces. Simundic (1997) tested a series of diaphragm H-shaped walls with various types of connectors. Lissel et al. (2000) evaluated the influence of the type of ties used in interconnected block-work diaphragm walls. Furthermore, Bosiljkov et al. (2004) developed an analytical study based on Simundic's experiments using a complex Finite Element model to simulate the specimens' behaviour. After studying the interaction of clay block-work H-shaped walls subjected to vertical loading, Capuzzo (2000) developed a research project at the University of São Paulo to further analyse this subject. This study includes a proposed test to assess the shear strength of vertical interfaces of interconnected masonry walls. More details can be found in Capuzzo et al.(2007) and Capuzzo (2005).

This paper describes an experimental program to shed light on the structural interaction of running bond interconnected walls subjected to vertical loading. The experimental work was carried out with third-scale symmetrical H-panels, with a top course bond beam, considering different sets of dimensions and the existence of a reinforced concrete slab on the top in order to evaluate their influence on the load capacity of the walls.

PROPERTIES OF THE MATERIALS

Blocks

All the tests were carried out using third scale models to make the test apparatus and procedures easier, cheaper and viable. The validity of this and the scale factors for the natural scale were previously cited by Capuzzo (2005).

The third-scale clay block dimensions are shown in Table 1. Table 2 presents the average results for compressive and tensile strengths and the Young modulus of the blocks. All of them are referred to as the net area.

Table 1. Geometrical dimensions of third-scale blocks

<table>
<tr><td rowspan="4">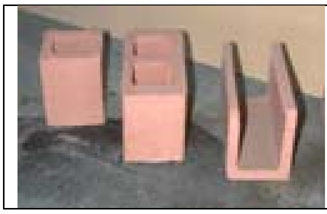</td><th>Type of block</th><th>Thickness (mm)</th><th>Length (mm)</th><th>Height (mm)</th></tr>
<tr><td>Block</td><td>47</td><td>97</td><td>63</td></tr>
<tr><td>Half Block</td><td>47</td><td>47</td><td>63</td></tr>
<tr><td>U-block</td><td>47</td><td>97</td><td>63</td></tr>
</table>

Table 2. Mechanical properties of third-scale blocks

Compressive strength (MPa)	Indirect tensile strength (MPa)	Young modulus (GPa)
59.83	5.91	22.0

Mortar, grout and concrete

The adopted mortar mix proportion was 1:0.5:4.5 (cement, lime and sand), by volume, and a water/cement ratio of 1.21. Very fine sand was used to keep the maximum grain dimension beyond the limit of one third of the bed and the thickness of the head joints, which was 3mm. Three cylindrical mortar specimens (50mm x 100mm) were built to measure the compressive strength and the Young modulus, whose average values were 6.8 MPa and 10.0 GPa, respectively.

The mass proportion of the grout used to fill the top course U-blocks was 1:0.76:1.26 (cement: sand: gravel) with a water/cement ratio of 0.37 and an addition of 0.7% of a super plasticizer. Three cylindrical mortar specimens (50mm x 100mm) were cast to evaluate the compressive strength and the Young modulus, whose average values were 49.7 MPa and 27.9 GPa, correspondingly. Strong grout was chosen to match the compressive strength of the clay blocks (see Table 2).

The concrete for the base and top slab was cast with a mass proportion of 1:1.99:2.06 (cement: sand: gravel) and a water/cement ratio of 0.65. The average results for the compressive strength and the Young modulus of three cylindrical specimens (50mm x 100mm) were 29.7 MPa and 25.4 GPa, in that order.

Reinforcement of the Bond Beam and the Slabs

One steel bar of 4.2mm diameter and a 600 N/mm^2 yield limit was inserted into each bond beam.

The top slab was built with a thickness of 35 mm, and reinforced with a mesh of 98 mm^2/m on both faces. It was bedded on the top course using the same mortar, which was already described. A base slab was also provided to transport the panels. Its height was 50mm and the double face reinforcing mesh was high, 240 mm^2/m, to avoid its failure during the tests and transportation procedures.

DESCRIPTION OF THE TESTED MASONRY PANELS

Geometry of the Panels

The choice of the panel dimensions was based on Corrêa and Page (2001), who studied the homogenization of the vertical compressive stresses. The referred authors proposed that Saint Venant's Principle governs the homogenisation process for concentric loading and that the vertical distance needed to reach homogenisation must be larger than the diameter of the circle that circumscribes the intersecting walls in plan view.

All the panels consisted of three bonded walls, built with an H symmetrical shape to reduce eccentricities and with a height of 792mm. Two different situations were considered, keeping the same proportion between the flange and the web lengths (83%). In the first one (see Figure1a), the diameter of the circle that circumscribes the panel in plain view was 460mm, smaller than the panel's height (50%), which allows for the stress homogenization to occur. In the second situation (see Figure1b), the aforementioned diameter was 1220mm, larger than the distance between the base and top slab (154%), which is not enough to reach the total stress homogenization.

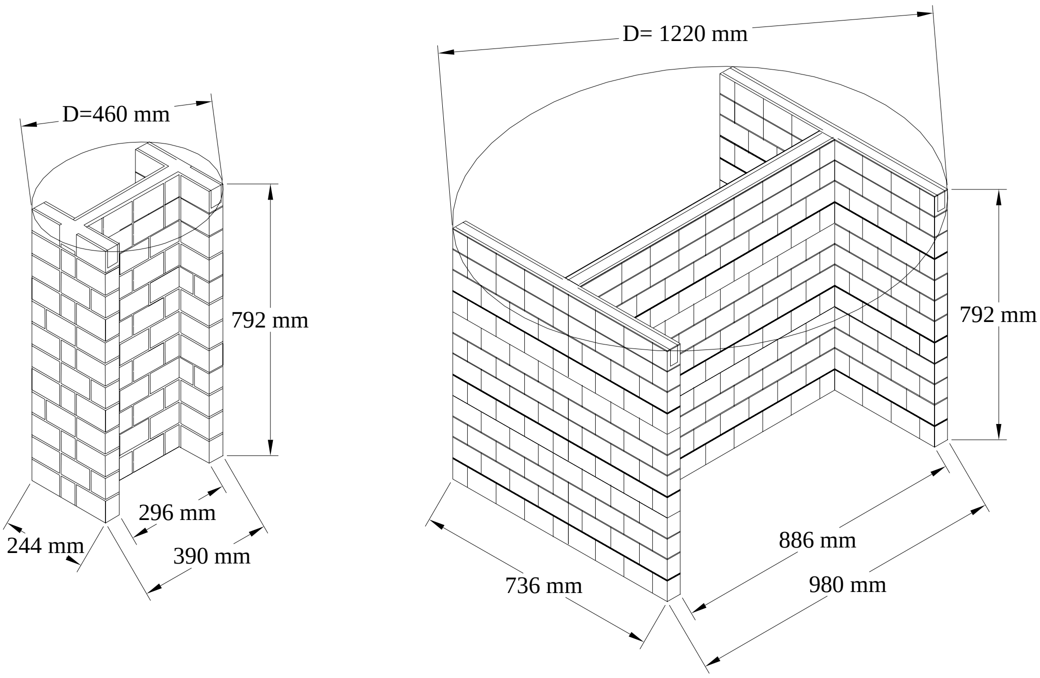

Figure 1. Geometry of the panels

Influence of the Top Slab

In order to represent a panel that is part of a building structure, the study considered the influence of a top slab, which partially constrains the flange bending that happens when the web wall is vertically loaded. For each set of dimensions, two different panels were tested, one with and the other without a top slab, totalizing four panels. All panels had a top bond beam and were vertically loaded only on the web wall to study the liable transference of force from the web to the flanges. The whole base of the panels (web and flanges) was supported by the base slab. Figure 2 illustrates the 4 panels, showing the symbols adopted to identify them.

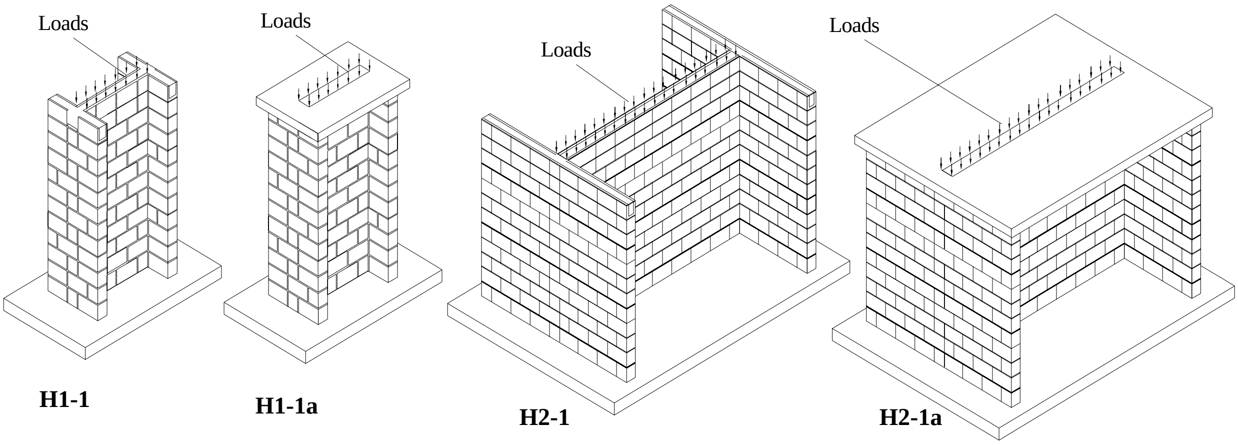

Figure 2. The four tested panels

TESTING PROCEDURES

All the tests were carried out in a servo controlled hydraulic jack with an initial speed of 0.01mm/s, reduced to 0.001mm/s near the failure load. Vertical loads were applied to the web top. The web and flange bases were supported. A few initial cycles of small vertical loads were applied in order to bed in the specimens and check the instrumentation. To confirm the force transference, a set of gauges were placed on the flanges and web at two different levels (near the top and near the base) to register strains. SYSTEM 5000 was used to automatically read and record data. Figures 3 and 4 show the test apparatus for panels type H1 and H2, respectively.

EXPERIMENTAL RESULTS

Table 3 shows the results related to the four panels: the failure load, the corresponding compressive stresses referred to two alternative areas and the compressive strength of wallets. These wallets were built by the same expert bricklayer and with the same materials of the panels, with a length of 4 blocks and a height of 5 courses. On one hand, consider the compressive stresses at failure for panels H1-1 and H2-1. Note that both do not have a top slab. When the stresses were assessed considering only the cross sectional area of the web wall, the obtained values were nearly the same (8.90 and 8.80 MPa), and only 18% larger than the masonry compressive strength, evaluated by the test of wallets (7.49 MPa). On the other hand, taking into account the whole base cross sectional area (web plus flanges) the compressive stresses dropped to 3.33 MPa, much smaller than the wallets strength. Therefore it is apparent that the contribution of the flanges to the load capacity of the panel was relatively low in this case.

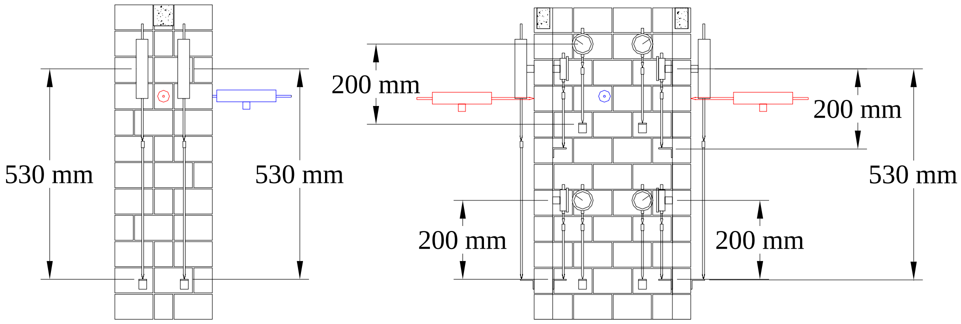

Front-view Side-view

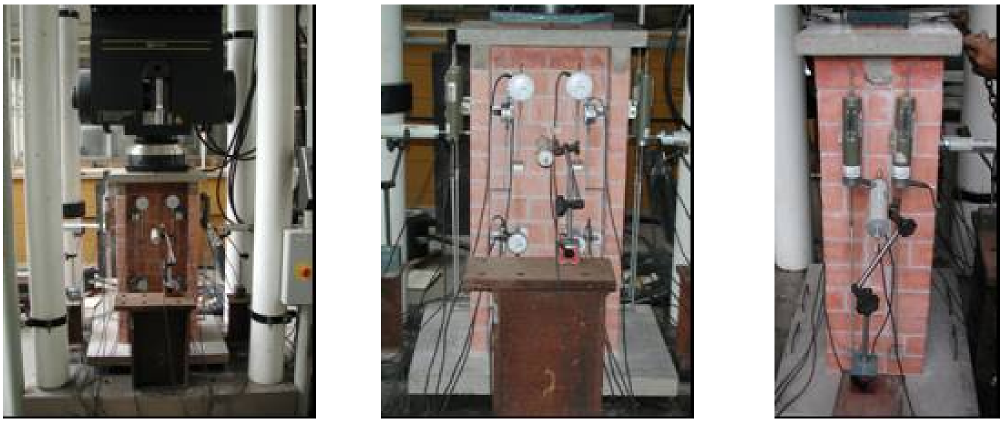

General view **Web wall** **Flange wall**

Figure 3. Test apparatus for panels H1

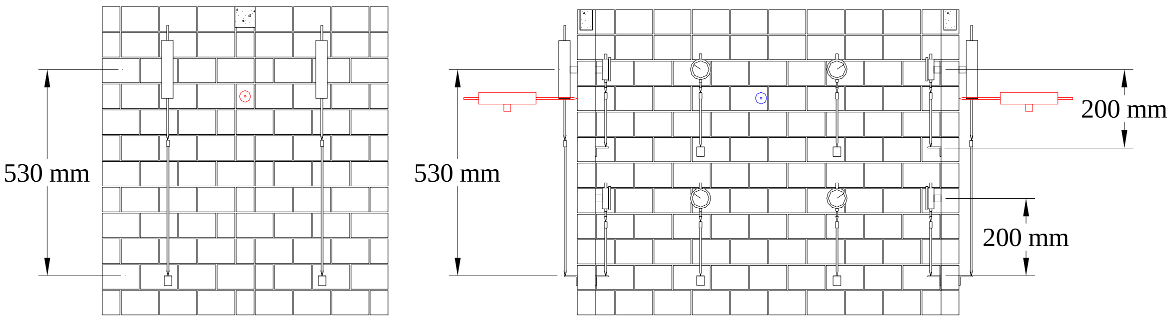

Front-view Side-view

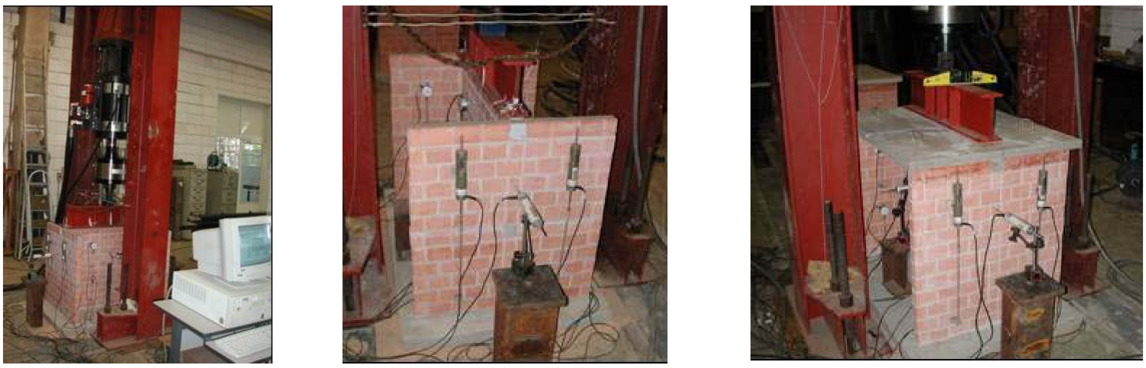

Figure 4. Test apparatus for panels H2

Panels H1-1a and H2-1a, which have a top slab, show different behaviours. In this case, the compressive stresses at failure which referred to the cross sectional area of only the web wall

Table 3. Experimental results for panels H1-1, H1-1a, H2-1 and H2-1a

Panel	Failure load (kN)	Failure compressive stress [1] (MPa)	Failure compressive stress [2] (MPa)	Compressive strength of wallets[3] (MPa)
H1-1	121.32	8.90	3.33	7.49
H1-1a	166.18	12.19	4.56	7.49
H2-1	367.15	8.88	3.33	7.49
H2-1a	467.05	11.29	4.23	7.49

[1] Referred to web wall area in plan view;
[2] Referred to the whole base area in plan view (web plus flanges);
[3] Wallets of a length of 4 blocks and a height of 5 courses;
Obs: All the results related to the gross area.

were at least 50% larger than the wallet strength (7.49 MPa). Note that the stresses which referred to the whole area (web plus flanges) showed a difference of 40% to the wallet strength. It is apparent that the flanges contributed considerably to the load capacity of the H panel, which was related to the existence of the top slab. This changed the way failure occurred, as later discussed in this section. It is worth mentioning that the contribution of the flanges could be clearly observed, even applying the load only to the top of the web wall.

The results of the strains were averaged taking into account groups of instruments to ease the analysis of the panel behaviour. Each group was defined depending on the position of the instrument. The instruments on the web defined two groups: the higher web and lower web. The instruments positioned on the internal face of the flanges were grouped in: higher flange and lower flange. As there was only one configuration on the external flanges, the instruments were grouped only as an external flange. Figure 5 shows the force-strain curves for all the panels. Note that the obtained results for the horizontal instruments were omitted because all of them were smaller than 0.5 mm and used only with the aim of providing subsidiary control.

Figures 5a and 5b show that the global behaviours of panels H1-1 and H1-1a were similar to a vertical load of nearly 100 kN. As well as this value, there was a force relief in the flanges, up to the peak value of 122 kN (Figure 5.a). However, in panel H1-1a, which has a top slab, there was instability near 120 kN. The panel showed an extra load capacity, after that value, reaching the peak load of 166 kN (Figure 5.b). During the last step, the strains in the higher flange group enlarged, while the strains in the external and lower flange group stayed nearly constant. It is apparent that the stress homogenization happened near the base of both panels H1-1 and H1-1a, since the strains in the lower flange and lower web were similar.

The behaviour of panels H2-1 and H2-1a can be observed in Figures 5c and 5d. The differences of the strains at the higher and lower levels were larger in panel H2-1 compared to panel H2-1a, which had the top slab. Regarding the flanges, there was a large bending effect in panel H2-1 because of the lack of the top slab. That effect was observed even at the beginning of the test, as can be seen by the positive strains in the external flange group (see Figure 5c). In the other panel, the constraint of the top slab kept the external flange strains negative, i.e., associated to compressive stresses, up to the intensification of the vertical interface cracking. Afterward the flexure became dominant in the flanges and the external strains changed signals, showing evidence that there was tension on the external face. For these panels the homogenization process is low, with large differences between the strains in the flanges and web at inferior levels, as expected by means of the Saint Venant’s Principle.

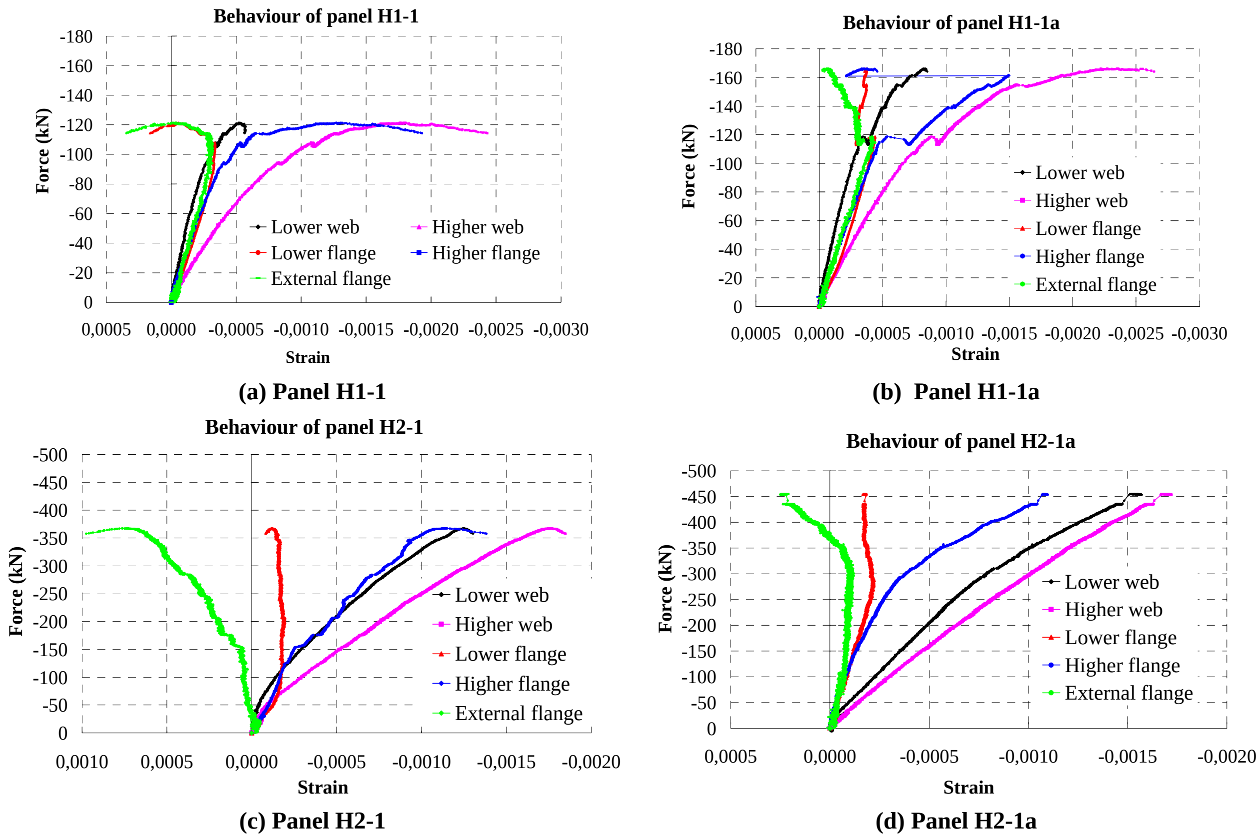

Figure 5. Force-strain graphs for panels H1-1, H1-1a, H2-1 and H2-1a

The existence of the top slab caused changes in the behaviour of the panels H1, as can be seen in Figure 6. In panel H1-1, which did not have a top slab, the cracks were predominantly concentrated near the vertical interfaces (Figure 6a). On the other hand, panel H1-1a, which has a top slab beside the cracks near the vertical interfaces, showed vertical cracks scattered on the walls, which are typically related to compressive failure. Panels H2 showed severe inclined cracks near the vertical interfaces, caused by shear stresses that induced the separation between the web and flanges. After the separating, the entire additional vertical load was supported by the web wall up to its compressive failure. Note that in the case of panel H2-1a, a brittle failure could not be avoided (Figure 6d), even applying the load with displacement control.

The comparisons of peak loads corresponding to panels that have the same dimensions highlight the influence of the top slab. In Table 4 the results are summarised, including the ratio of the peak loads referred to the panel without a top slab. Note that the existence of the top slab in panels H1 enlarged 37% the peak load, while the increase was 27% for panels H2. Panels H1-1 and H2-1, which did not have a top slab, showed a severe cracking distribution close to the vertical interfaces, leading to a consequent relief of the flanges and the predominant support of the web wall. Therefore, the load capacity of the panels without a top slab was largely dependent on the compressive strength of the web wall. Panels H1-1a and H2-1a that had a top slab also showed intense cracks near the vertical interfaces. Nevertheless, the top slab did not allow a large relief of the flange walls, which continued to hold up large amounts of the vertical load up to the end of the test. Consequently, the load capacity of the H-panel was a combination of large contributions of both web and flange walls, without a predominance of the web.

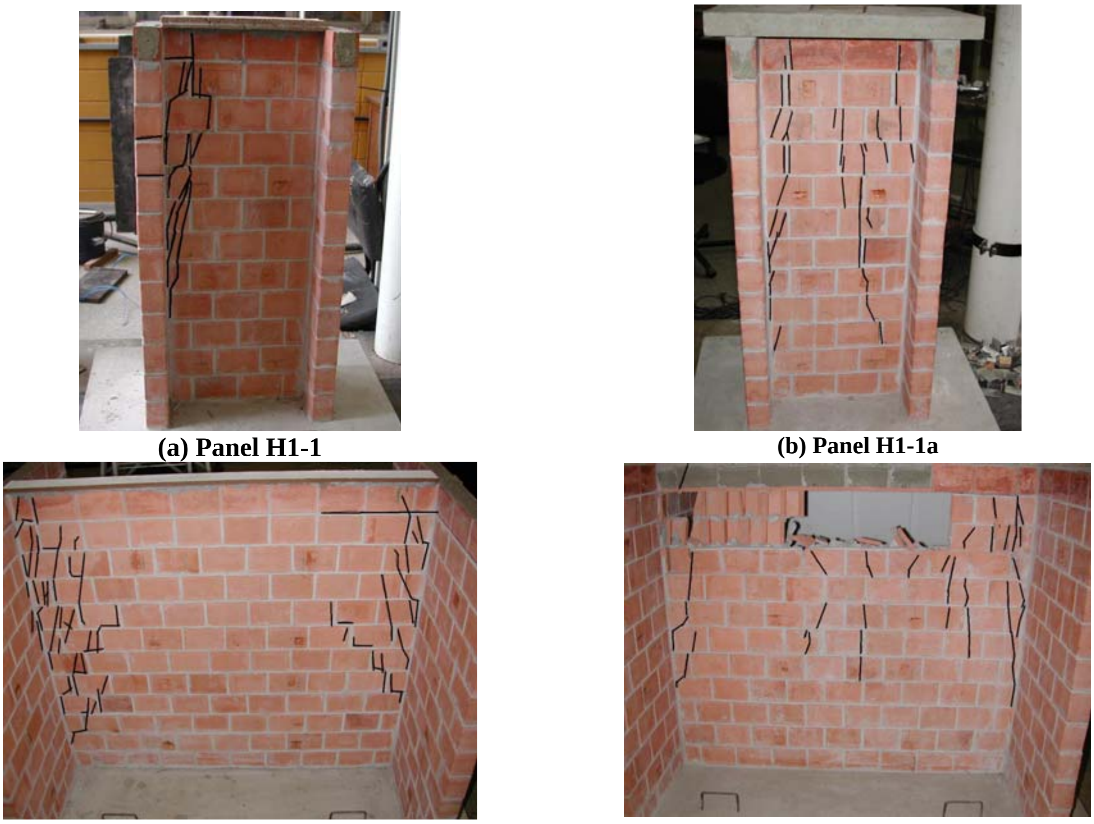

(a) Panel H1-1 (b) Panel H1-1a (c) Panel H2-1 (d) Panel H2-1a

Figure 6. Comparison of failure patterns for panels H1-1, H1-1a, H2-1 and H2-1a

Table 4. Comparison of failure loads for H1 and H2

Type of panel	Failure load (kN)	Ratio to H1-1	Type of panel	Failure load (kN)	Ratio to H2-1
H1-1 (without top slab)	121.32	1.00	H2-1 (without top slab)	367.15	1.00
H1-1a (with top slab)	166.18	1.37	H2-1a (with top slab)	467.05	1.27

Figure 7 shows details of the graphs already displayed in Figure 5, focusing on the linear parts and only for the web walls. Comparing panels H1-1 (without top slab) and H1-1a (with the top slab) the similarity of the behaviours is apparent, as seen in Figures 7a and 7b. The lines had slopes that differ only 13% (Figure 7c), which suggests that the influence of the slab was short for small loads. The transference of force from the web to the flange walls was noticeable since the strains in the lower levels of the wall were smaller than those near the top. The linear parts of the graphs of panel H2-1 had slopes that differ 56% (Figure 7d), and the superior strains were higher. This difference was smaller for panel H2-1a, 28%, showing that the force transference from the web to the flange was larger in this case, probably because part of the vertical load flowed directly to the flanges through the slab, before it compressed the top of the web wall.

Figure 8 shows details of the linear parts of the graphs corresponding to the flanges. The similarity of the slopes of Figures 8a and 8b confirms that the slab had a limited influence on panel H1 for small loads. Figures 8c and 8d show results for panel H2. Despite some oscillation on the results, especially for the external flange instruments, the influence of the

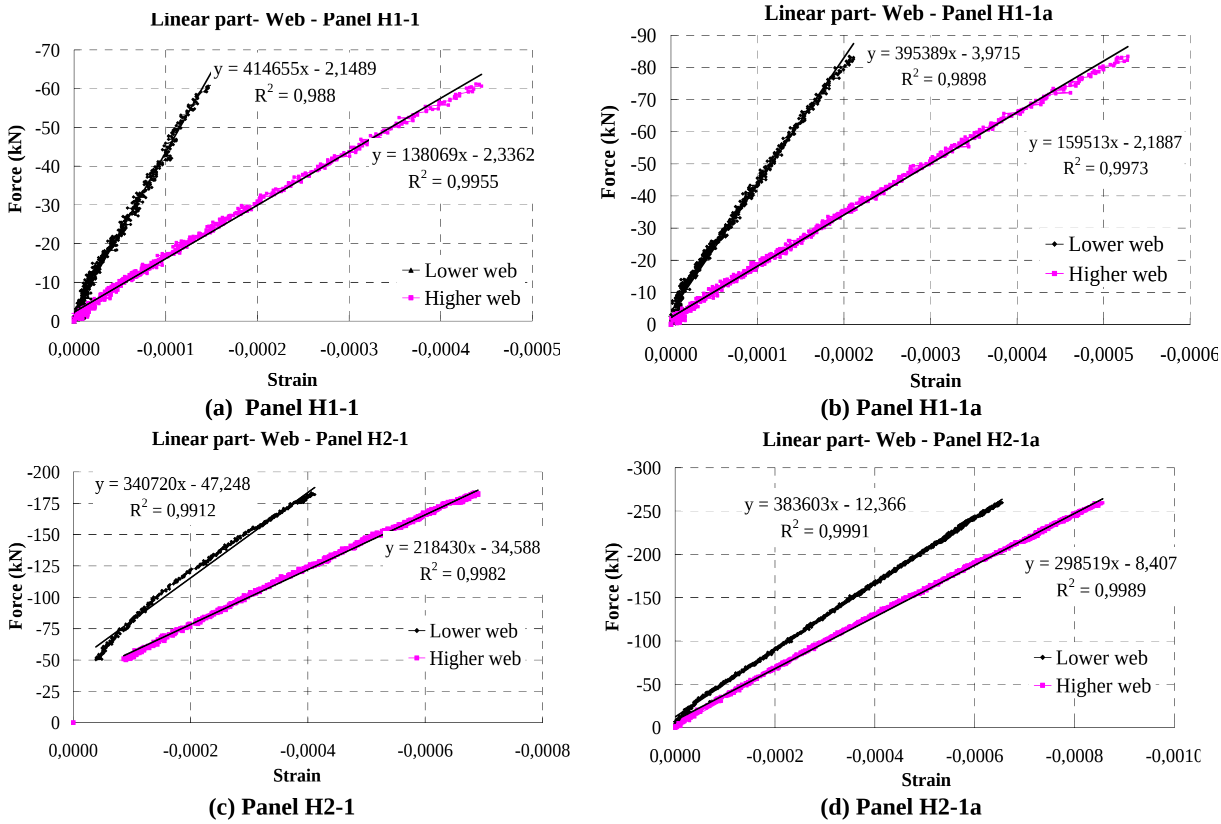

Figure 7. Comparison of how the strains changed in the web walls for panels H1 and H2

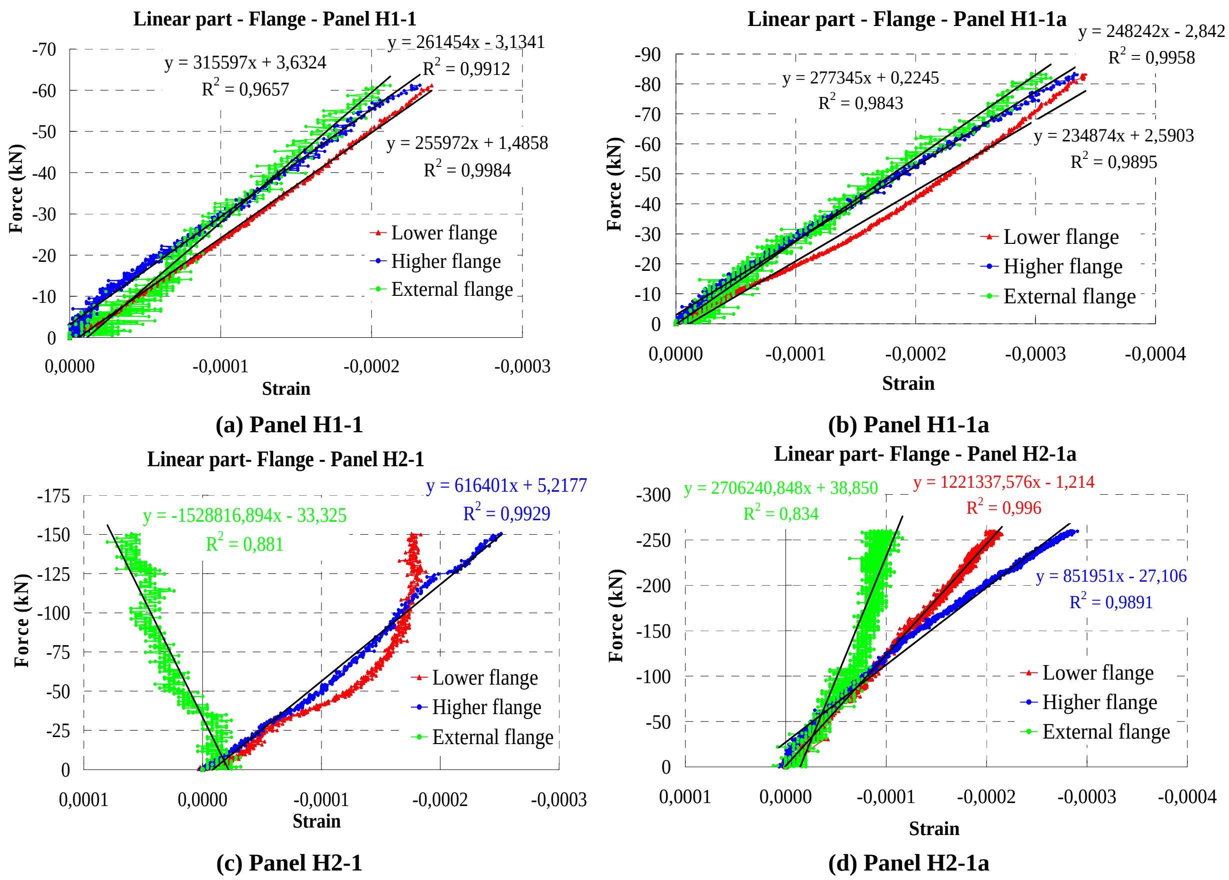

Figure 8. Comparison of how the strains changed in the flange walls for panels H1 and H2

top slab is apparent as the graphs for panels H2-1 and H2-1a are different. The external flanges in panel H2-1a were always compressed, while they showed a significant bending in panel H2-1, because there was no top slab to constrain it.

PRELIMINARY CONCLUSIONS

The main conclusions of the paper based on the experimental results are:

- Saint Venant's Principle is a helpful tool to consider the possibility of stress homogenization in a set of interconnected masonry walls.
- the existence of a top slab was beneficial for the increase of the load capacity of the tested walls; the enlargement of the failure load was roughly 30% in the studied cases, compared to the results for corresponding panels with and without a top slab;
- the influence of the top slab was related to a restriction of the bending of the flange walls and the possibility of direct force transfer from the top of the web to the flange walls;
- another influence of the slab is the prolongation of the linear paths of the graphs.

ACKNOWLEDGEMENTS

The authors gratefully acknowledge the support of FAPESP and CNPq.

REFERENCES

Bosiljkov, V.; Simundic, G.; Page, A.W. "An analytical study of the composite behaviour of masonry geometric sections." *Proceedings of the 7th Australian Masonry Conference,* Newcastle, NSW, 2004. pp. 466-475.

Corrêa, M.R.S.; Page, A.W. "The Interaction of Load-Bearing Masonry Walls Subjected to Vertical Loads". *Res. Report No. 218.12.2001*. The University of Newcastle. Australia. 2001.

Capuzzo Neto, V. "Theoretical and experimental study of the interaction of interconnected walls subjected to vertical loads." São Carlos, 2000. 111p. *M.Sc. Dissertation – School of Engineering of São Carlos. University of São Paulo*. (In Portuguese)

Capuzzo Neto. V. "Interaction of interconnected clay masonry walls subjected to vertical loads. " São Carlos, 2005. 321p. *PhD Thesis – School of Engineering of São Carlos. University of São Paulo.* (in Portuguese)

Capuzzo Neto, V.; Corrêa, M.R.S.; Ramalho, M.A. "Shear strength of vertical interfaces of intersecting walls", 2007. *Proceedings of the 10th North American Masonry Conference*, St. Louis, MO, pp. 872-883.

Lissel, S.L.; Shrive, N.G.; Page; A.W. "Shear in plain, bed joint reinforced, and post-tensioned masonry". *Canadian Journal of Civil Engineering*, 2000, 27 (5): 1021-1030.

Simundic, G. "Diaphragm walls." 1997. *M.Sc. Dissertation. University of Newcastle*, New South Wales, Australia.